RESEARCH ARTICLE | OCTOBER 18 2024

Low uncertainty thermodynamic temperature above the silver point using relative primary radiometry

D. Lowe **□**; G. Machin

AIP Conf. Proc. 3230, 100002 (2024) https://doi.org/10.1063/5.0234817







Low Uncertainty Thermodynamic Temperature Above the Silver Point Using Relative Primary Radiometry

D. Lowe^{1, a)} and G. Machin¹

¹National Physical Laboratory, Teddington UK TW11 0LW

^{a)}Corresponding author: dave.lowe@npl.co.uk

Abstract. The *mise-en-pratique* for the definition of the kelvin has given the possibility of relative primary thermometry with uncertainties competitive with the ITS-90 above the silver freezing point. The *mise-en-pratique* does not constrain users to any particular experimental method to realise the kelvin, so while there is supporting documentation it may not be obvious to everyone how to actually establish SI traceable temperatures. NPL has established thermodynamic temperature above the silver point using high-temperature fixed-points. This approach provides access to thermodynamic temperature with lower uncertainties than can be routinely achieved through absolute primary radiometry. We demonstrate direct traceability to the kelvin and that this is more easily and robustly achieved than its equivalent ITS-90 approximation.

INTRODUCTION

National Measurement Institutes generally disseminate temperature through the International Temperature Scale of 1990 (ITS-90) [1]. It is a good approximation and has always been an easier approach to establishing traceability than by thermodynamic means. However, there are conceptual issues with ITS-90. While it is specified that the degree Celsius differs from the kelvin by a constant amount it is clear from values of T-T90 that the temperature unit of ITS-90 has different magnitude depending upon which temperature is being measured. Also, there are some parts of the scale that have multiple definitions. For example, above the silver freezing point (961.78 °C) depending on which reference fixed-point blackbody is used (Ag, Au or Cu) three different versions of the ITS-90 can be established (though they should all be formally equivalent within the uncertainties).

For most users the practical advantages of using the defined scale outweigh these issues. However, at higher temperatures above the freezing point of silver things are a bit different since with the adoption of the *mise-en-pratique* for the definition of the kelvin (*MeP*-K) [2,3] establishing thermodynamic temperature by relative primary radiometry might be easier and more robust than setting up an ITS-90 realisation [3]. Here, we examine how using the relative primary radiometric thermometry route laid out within the *MeP*-K compares with the results one typically obtains using absolute primary radiometry. The emphasis will be on what was done at each step of establishing thermodynamic temperatures by relative primary radiometry so as to help develop a practical "user" guide through worked example. The NPL relative primary radiometry thermodynamic temperatures used here were established as part of assigning thermodynamic temperature to a series of high temperature fixed point (HTFP) blackbodies [4] from 1465 K to 3020 K as part of the Realising the Redefined Kelvin (Real-K) project [5].

The *MeP*-K-19

The stated purpose of the *MeP*-K is to "indicate how the definition of the SI base unit, the kelvin, symbol K, may be realised in practice" [2]. Section 4.2.3 "Relative primary radiometric thermometry" lists extrapolation from one fixed-point and interpolation (and if necessary, extrapolation) using two, three or more fixed points of known thermodynamic temperature. A supporting document of the *MeP*-K lists values and uncertainties for high temperature fixed-points (HTFPs) [6], and these, as well as the published thermodynamic temperatures of the ITS-90 defining

fixed points (Ag, Au or Cu) can be used to establish thermodynamic temperature values by relative primary radiometry. The necessary fitting equations (the *MeP*-K-19 suggests the Planck form of the Sakuma-Hattori equation, given in [8]) and sensitivity coefficients are helpfully already published [9].

Requirements of ITS-90 compared to thermodynamic temperature above the silver point

To establish the ITS-90, T_{90} , above the silver freezing point requires a silver, gold or copper fixed-point blackbody. NPL uses a copper fixed-point blackbody in a 3-zone tube furnace. A linear radiation thermometer extrapolates from the copper freezing point (approximately 1084 °C) up to 3000 °C. This thermometer needs periodic calibration of its interference filters, (which define its operating wavelength) to establish and maintain ITS-90 with reasonable uncertainty. The linearity of the silicon photodiode detector also needs to be periodically determined and corrected for. The ITS-90 is then disseminated by calibrating customer non-contact thermometers by comparison to this linear thermometer using a variable high temperature blackbody.

To establish thermodynamic temperature, T, by relative primary radiometry one or more fixed points with known thermodynamic temperature are required [6]. At NPL, the high temperature blackbody source used for scale dissemination can also be used for realising the HTFPs with minor modification [10]. The same linear radiation thermometer is then calibrated at two or three HTFPs without the need for its spectral response to be known and then, as before, used with the high temperature blackbody for calibration of customer non-contact thermometers by comparison. But of course, in this case T not T_{90} is the result.

We will see below that the extra equipment needed for the uncertainty evaluation is the same for T and T_{90} , so at higher temperatures T can be realised more simply than T_{90} as spectral calibration is not needed, though an initial evaluation to ensure that the filters are narrow compared to the operating wavelength and blocked to avoid stray thermal radiation entering the detector needs to be performed.

Number of fixed points, n

The *MeP*-K gives n=2 and n=3 or more HTFPs as suitable for interpolation, but the supporting documentation [6] recommends n=2 where both interpolation and extrapolation is needed. The need here was for establishing thermodynamic temperature that could be extrapolated to the WC-C point at 3020 K, so n=2 was used. With a choice of Cu, Co-C, Pt-C and Re-C we could check the temperature performance of the various different proposed schemes against a baseline, in the case of figure 1 this was n=2 established using thermodynamic temperatures of Re-C [6]and Cu [1, 6] compared to other indicated schemes.

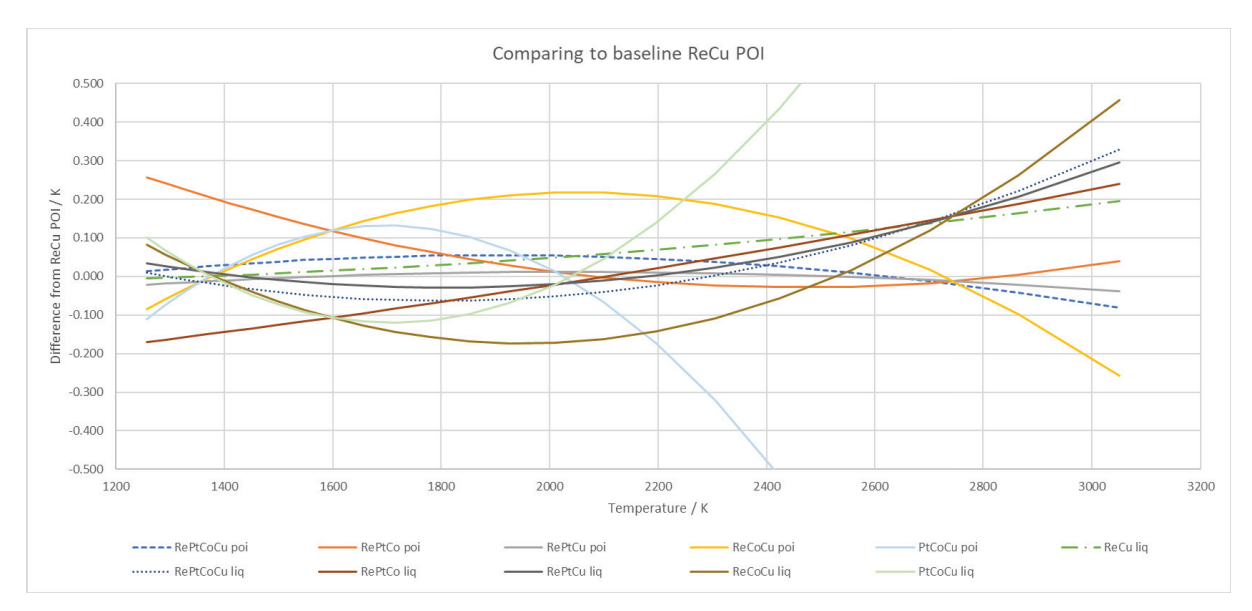


FIGURE 1. Change in thermodynamic temperature from the baseline, established by Re-C and Cu (n=2), for different schemes and fixed-point choice

From Fig. 1, n=3(RePtCo) has a larger than acceptable error extrapolating down to Cu (much larger than any uncertainty). For n=3(ReCoCu) agreement to the fit at Co is poor and has a large error near the not used Pt-C, and finally n=3(PtCoCu) again doesn't fit well at Co and diverges rapidly extrapolating above Pt-C, giving an unreasonably large error at Re-C. From this analysis it was concluded that measurements we made at the Co-C (~1597 K) were suspect, perhaps due to high levels of impurities. In other respects, there was little difference in the performance of the fit no matter which HTFPs or which n was used. Using n=3 (RePtCu) or n=4 (RePtCoCu) and checking agreement with n=2 ensures very robust establishment of thermodynamic temperature, staying within ±0.2 °C over the whole range.

Choice of defined temperature

The MeP-K lists thermodynamic temperature values for the point-of-inflection (POI) and the liquidus point (LIQ) for the HTFPs. As commented on in [11], to use the POI requires that an arbitrary HTFP blackbody has some link to the HTFPs used in defining the POI value, or at least has been through a similar selection process to the original HTFPs. Using the liquidus point avoids this issue as it is a definable thermodynamic event. However, it is less easy to identify the liquidus point than the POI which consequently leads to somewhat larger overall uncertainty, depending on the melting range of the HTFP. In the measurements performed here there was a direct link to previous measurements by a selection process [12], and so the POI was used.

Calibration of non-contact thermometer Signal versus Temperature

The Sakuma-Hattori equation has a term related to the instrument responsivity and two terms relating to spectral response (as well as a requirement that it is narrow bandpass [8]). One of the two relates to the central wavelength and the other to the width and shape of the bandpass. Calibration based on signal-temperature measurements (i.e., no spectral calibration) therefore requires three measurements. The n=2 approach works because a reasonable estimate of the filter shape and bandpass can still give acceptable results. The relevant equations are given in [13]. In this case the radiometer¹ filter is specified as 10 nm full width half maximum (fwhm). We have measured what is nominally the same filter as 14 nm fwhm and as having between a Gaussian and rectangular shape. From this, we use the average as the parameter σ and the limits as $\delta\sigma$. The equation for n=2 is [13]

$$S = \frac{a_1}{exp[\lambda_0(1 - 6\sigma^2/\lambda_0^2)T + c_2\sigma^2/2\lambda_0^2] - 1}$$
 (1)

where c_2 is the second radiation constant. To ensure the link is with thermodynamic temperature we use the value of the second radiation constant calculated from the defined values of h, c and k_B , this value is 1.438 776 877...× 10⁻² m K with no uncertainty as the defined values have no uncertainty. Other terms are, a_I is an instrument specific constant and λ_0 is the central wavelength of the radiometer. (1) can be rewritten to remove a_1

$$S_1(\exp[c_2/\lambda_0(1-6\sigma^2/\lambda_0^2)T_1+c_2\sigma^2/2\lambda_0^2]-1) = S_2(\exp[c_2/\lambda_0(1-6\sigma^2/\lambda_0^2)T_2+c_2\sigma^2/2\lambda_0^2]-1)$$
(2)

where $S_{1,2}$ are the measured radiances of the fixed points with known temperatures $T_{1,2}$. To solve this for λ_0 we plotted the difference between LHS and RHS and found the minimum, and with λ_0 find a_1 from (1).

The inverse of the Sakuma-Hattori equation (i.e., to get a temperature given a signal) is [9]

$$T = \frac{c_2}{a_2 \ln\left(\frac{a_1}{S} + 1\right)} - \frac{a_3}{a_2} \tag{3}$$

The constant a_1 already known, a_2 and a_3 can be found from $a_2 = \lambda_0 (1 - 6 \sigma^2 / \lambda_0^2)$ and $a_3 = c_2 \sigma^2 / 2 \lambda_0^2$ as given in [13] and repeated here for convenience.

¹ We use the word radiometer for a radiation thermometer used for thermodynamic radiance measurement

Measurement of fixed-point cells

The calibration of the linear radiation thermometer consisted of measurement of the melting curves of two fixed-point blackbodies. These were a rhenium-carbon HTFP installed in a single-zone high-temperature furnace [14] and the NPL copper-point standard blackbody in a three-zone furnace [15]. The signal at the copper point used was the photocurrent during the freeze. For the Re-C the signal used was the photocurrent of the POI of the melting curve. Iteration of a cubic function fit [16] was used to identify this value. The specified limits approach [17] could be used if the scale were to be based on the liquidus. The measured radiance (photocurrent) was corrected for the calculated emissivity of the fixed-point cell.

From the above measurements we now have an evaluated value for σ , measurement photocurrents S_1 and S_2 and given temperatures T_1 and T_2 , and we need to establish uncertainties for each of these.

UNCERTAINTY BUDGET

As described above, different interference filter spectral responses (part measured, part manufacturers specification) were used to calculate values for σ and the mid-point and limits were used for σ and $\delta \sigma$. Below we step through the establishment of the measurement uncertainties.

The photocurrent uncertainties were made up of

- blackbody emissivity this was calculated using NPL written software [18]. Half was applied as a correction and half as an uncertainty.
- size-of-source effect (SSE) the measured response to signal outside the nominal field-of-view allows for differences between the 3 mm cavity and the extended source of the furnace. To measure the SSE an integrating sphere with a suitable lamp and a 50 mm diameter port was used, with central 3 mm blocked and various diameter apertures [19]
- gain ratio taken from measurements of HTFPs at different gain settings
- non-linearity taken to be within measured limits of $5x10^{-4}$ fraction of the signal. Uses a stable reference radiance source with a double aperture on the linear radiation thermometer
- repeatability of the calibration measurements

No allowance was made for ambient effects: the linear radiation thermometer itself is temperature stabilised and is used in a laboratory that is controlled within 0.2 °C.

The temperature uncertainties were made up of

- value of the HTFP either the uncertainty given in [6] or the uncertainty in T- T_{90} [7]
- impurities for copper, which has been part of intercomparisons, a "normal" value was used from [20]. Rhenium-carbon used comparisons including NPL made cells as part of defining HTFP values [11, 12]
- cavity temperature drop the change in temperature across the cavity wall was taken from published recommendations; for copper [20] and [21] for rhenium-carbon. In principle this could be at least partly corrected, but here it was just taken as an uncertainty
- identification of phase transition recommended "normal" value for copper [20] and from [16] for rhenium-carbon
- furnace effect only applied to rhenium-carbon as recommended [22].

Evaluating how these components propagate has been given elsewhere [9] so here we just use the relevant equations to combine everything into an uncertainty for the linear radiation thermometer at any temperature. This is the "scale realisation uncertainty" and needs to be combined with any allowance for drift together with uncertainties arising from actual use to assign a temperature – the "in-use" uncertainty.

The stability of the linear radiation thermometer was assessed over the approximately six-month period from the initial calibration, the measurement campaign and then instrument re-calibration. It proved very stable and a fixed 27 mK was applied to the in-use uncertainties as a component for drift.

These components were combined in quadrature to give the scale realisation uncertainty of the linear radiation thermometer.

THERMODYNAMIC TEMPERATURE ASSIGNMENT

Part of Euramet project Realising the redefined kelvin "Real-K" [5] aims to add more HTFPs whose thermodynamic temperature are known with low uncertainty to the *MeP*-K annex [6]. Fixed-point blackbodies of Fe-C, Pd-C, Ru-C and WC-C were circulated to partners and measured to have thermodynamic temperatures assigned to their respective point-of-inflection and liquidus points. Final details of the *T* assignment are still to be published [23]. Here we look just at the magnitude of the NPL uncertainties, evaluated as per the process described in the previous section, and how they compare to other, previous, *T* assignment campaigns (for Co-C, Pt-C and Re-C). In particular, we look at measurements made before the adoption of HTFPs with low uncertainty temperatures for relative primary radiometry [24].

Figure 2 plots, as circles, the uncertainties reported by participating laboratories in assigning thermodynamic temperature values to Cu, Co-C, Pt-C and Re-C [11,16]. Alongside, as triangles, are the uncertainties we derive here when assigning thermodynamic temperatures to the fixed-point blackbodies as part of Real-K, i.e., through the combination of the scale realisation uncertainty, drift and the in-use uncertainty; emissivity, temperature drop, size-of-source, gain ratio, non-linearity and repeatability.

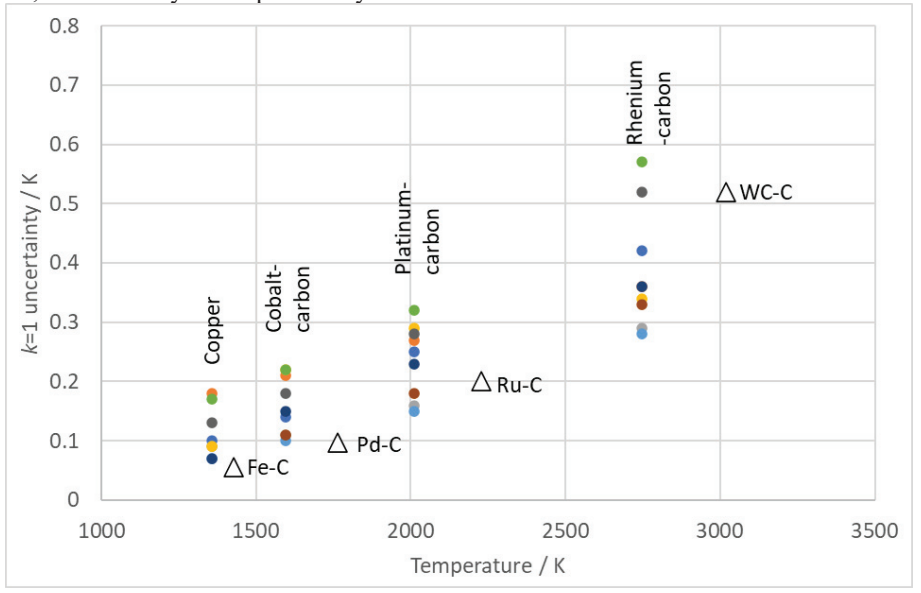


FIGURE 2. Comparative uncertainties – values assigned by direct primary radiometry to HTFP blackbodies [11, 16] and those reported here assigned by relative primary radiometry using *a priori* known HTFP values as the basis for the thermodynamic temperature assignment. Circles show individual laboratories uncertainty assigning *T* to Cu (1358 K), Co-C (1597 K), Pt-C (2011 K) and Re-C (2748 K). The triangles show the NPL uncertainty as assigning T to Fe-C (1426 K) Pd-C (1765 K) Ru-C (2227 K) and WC-C (3021 K)

More recently, absolute primary radiometry derived thermodynamic temperature values have been published for Fe-C and Pd-C [25]. It is apparent from the uncertainty budget given there that the dominant components of absolute radiometry relate to spectral calibration and aperture dimensions. Neither of these are required using relative primary radiometry, making this approach for realisation of thermodynamic temperature straightforward and rapid and therefore a simple and cost-effective way for NMIs to obtain a low uncertainty radiance scale without the need to invest in full absolute primary radiometry capability.

CONCLUSION

Aspects of the application of relative primary thermometry to obtain low uncertainty thermodynamic temperature are non-intuitive. Here we have worked, step-by-step, through how NPL uses relative primary radiometry with HTFPs to derive low uncertainty thermodynamic temperatures in the hope that others will find our approach a useful model to follow. The resulting low uncertainties support the suggestion that realising and disseminating thermodynamic temperature values derived from this approach are certainly competitive with the equivalent ITS-90 values. While we used the n=2 scheme we did not find any significant differences in extrapolation compared to using higher numbers of fixed points (n=3 or n=4). This approach is self-checking and more robust than ITS-90 above the silver point. This is evidenced by the fact that by comparing the thermodynamic temperature realisations from use of different HTFPs we found that the Co-C point measurements were possibly in error and as such its results could be discounted. It is clear that the use of relative primary radiometry, coupled with HTFPs of known consensus temperatures, to obtain thermodynamic temperature values is a more robust and straightforward way to get such values than either ITS-90 (with corrections) or absolute primary radiometry, with uncertainties equivalent or lower than the alternative approaches.

ACKNOWLEDGEMENT

This paper has been written through funding received from the EU EMPIR programme co-financed by the Participating States and from the European Union's Horizon 2020 research and innovation programme, specifically from the EMPIR project 18SIB02 "Realising the redefined kelvin".

REFERENCES

- 1. H. Preston-Thomas, Metrologia 27 3 (1990).
- 2. SI Brochure 9th edition (2019) Appendix 2 (*MeP*-K-19) can be downloaded at: https://www.bipm.org/en/publications/mises-en-pratique
- 3. Machin, G., Bloembergen, P, Anhalt, K., Hartmann, J., Sadli, M., Saunders, P., Woolliams, E., Yamada, Y. & Yoon, H., "Practical implementation of the mise-en-pratique for the definition of the kelvin above the silver point", Int. J. Thermophys., 31, p. 1779-1788, DOI 10.1007/s10765-010-0834-5.
- 4. G. Machin, "Twelve years of high temperature fixed point research: a review" *AIP Conf. Proc.* **1552**, 305 (2013); doi: 10.1063/1.4821383.
- 5. G. Machin, M. Sadli, J. Pearce, J. Engert and R. Gavioso, Measurement 201 111725 (2022).
- 6. G. Machin, K. Anhalt, P. Bloembergen, S. Sadli, D. Lowe, P. Saunders, Y. Yamada, H. Yoon, "MEP-K RELATIVE PRIMARY RADIOMETRIC THERMOMETRY EDITION" (2017).
- 7. "Estimates of the Differences between Thermodynamic Temperature and the ITS-90", annex within [2].
- 8. F. Sakuma, M. Kobayashi, in Proceedings of TEMPMEKO '96, 6th International Symposium on Temperature and Thermal Measurements in Industry and Science, ed. by P. Marcarino (Levrotto and Bella, Torino, 1997), 305–310.
- 9. P. Saunders, Int. J. Thermophys. 32 26–44 (2011).
- 10. D. Lowe, L. Wright and C. Liller, "Improving fixed-point cell realization by modifying furnace heater shape" in *International Congress of Metrology* 24002 (2019).
- 11. E. Woolliams, K. Anhalt, M. Ballico, P. Bloembergen, F. Bourson, S. Briaudeau, J. Campos, M. G. Cox, D. del Campo, M. R. Dury, V. Gavrilov, I. Grigoryeva, M. L. Hernandez, F. Jahan, B. Khlevnoy, V. Khromchenko, D. H. Lowe, X. Lu, G. Machin, J. M. Mantilla, M. J. Martin, H. C. McEvoy, B. Rougié, M. Sadli, S. G. Salim, N. Sasajima, D. R. Taubert, A. Todd, R. Van den Bossche, E. van der Ham, T. Wang, D. Wei, A. Whittam, B. Wilthan, D. Woods, J. Woodward, Y. Yamada, Y. Yamaguchi, H. Yoon and Z. Yuan, Phil. Trans R. Soc. A. 374 20150044 (2016).
- 12. Y. Yamada, K. Anhalt, M. Battuello, P. Bloembergen, B. Khlevnoy, G. Machin, M. Matveyev, M. Sadli, A. Todd and T. J. Wang, Int. J. Thermophys. **36** 1834–1847 (2015).
- 13. P. Saunders and D. R. White, Metrologia 40 195–203 (2003).
- 14. Y. Yamada, N. Sasajima, H. Gomi, T. Sugai, (2003). High-Temperature Furnace Systems for Realizing Metal-Carbon Eutectic Fixed Points. AIP Conference Proceedings 684 985–990. 10.1063/1.1627257.
- 15. H C McEvoy, M Sadli, F Bourson, S Briaudeau and B Rougié, Metrologia 50 559 (2013).

- 16. D. H. Lowe, A. D. W. Todd, R. Van den Bossche, P. Bloembergen, K. Anhalt, M. Ballico, F. Bourson, S. Briaudeau, J. Campos, M. G. Cox, D. del Campo, M. Dury, V. Gavrilov, I. Grigoryeva, M. L. Hernanz, F. Jahan, B. Khlevnoy, V. Khromchenko, X. Lu, G. Machin, J. M. Mantilla, M. J. Martin, H. C. McEvoy, B. Rougié, M. Sadli, S. G. R. Salim, N. Sasajima, D. Taubert, E. van der Ham, T. Wang, D. Wei, A. Whittam, B. Wilthan, D. Woods, J. T. Woodward, E. R. Woolliams, Y. Yamada, Y. Yamaguchi, H. Yoon and Z. Yuan, Metrologia 54 390–398 (2017).
- 17. P. Bloembergen, W. Dong, C. Bai and T. Wang, Int. J. Thermophys. 32 2633–2656 (2011).
- 18. K. Berry, J. Phys. E: Sci. Instrum. 14 629–632 (1981).
- 19. G. Machin and R. Sergienko, "A comparative study of Size of Source Effect (SSE) Determination Techniques", In: Tempmeko 01, The 8th International Symposium on Temperature and Thermal Measurements in Industry and Science, Berlin, Germany, Eds. B Fellmuth, J. Seidel, & G. Scholz, Published: VDE VERLAG GMBH, p. 155 160 (2002).
- J. Fischer, M. Battuello, M. Sadli, M. Ballico, S. Nam Park, P. Saunders, B. C. Johnson, E. van der Ham, W. Li, F. Sakuma, G. Machin, N. Fox, S. Ugar and M. Matveyev, "Uncertainty budgets for realisation of scales by radiation thermometry" http://www.bipm.org/cc/CCT/Allowed/22/CCT03-03.pdf (2003).
- 21. P. Castro, G. Machin, P. Bloembergen and D. Lowe Int. J. Thermophys. **35** 1341–1352 (2015) DOI 10.1007/s10765-014-1677-2.
- 22. A. D. W. Todd, K. Anhalt, P. Bloembergen, B. Khlevnoy, D. H. Lowe, G. Machin, M. Sadli, N. Sasajima and P. Saunders, Metrologia **58** 035007 (2021).
- 23. M. Sadli, F. Bourson, D. Lowe, K. Anhalt, D. Taubert, M.J. Martin, J.M. Mantilla, F. Girard, M. Florio, C. Gözönünde, H. Nasibli, L. Kňazovická, N. Sasajima, X. Lu, O. Kozlova, S. Briaudeau and G. Machin, "Thermodynamic temperatures of Fe-C, Pd-C, Ru-C and WC-C for the mise-en-pratique of the kelvin up to 3020 K", In: these proceedings.
- 24. G. Machin, J. Engert, R. Gavioso, M. Sadli and E. Woolliams, Measurement 94 149-156 (2016).
- 25. M. J. Martin, J. M. Mantilla, C. Garcia-Izquierdo and D. del Campo, Int. J. Thermophys. 43 57 (2022).